J|A|C|S
ARTICLES
Published on Web 11/18/2003

# Synthesis of Amphiphilic Phenylazophenyl Glycosides and a Study of Their Liquid Crystal Properties

Nicolas Laurent,[†] Dominique Lafont,[†] Fabienne Dumoulin,[†] Paul Boullanger,*[,†] Grahame Mackenzie,[§] Paul H. J. Kouwer,[§] and John W. Goodby*[,§]

*Contribution from the Laboratoire de Chimie Organique II, Unité Mixte de Recherche CNRS 5181, Université Lyon 1, Chimie Physique Electronique de Lyon, 43 Bd du 11 Novembre 1918, F 69622 Villeurbanne, France, and Department of Chemistry, The University of Hull, Hull, HU6 7RX, U.K.*

Received July 17, 2003; E-mail: j.w.goodby@hull.ac.uk; p.boullanger@univ-lyon.fr

***Abstract:*** Several 4-(4′-*N*,*N*-didodecylaminophenylazo)phenyl 1,2-trans glycosides **5a**−**e** with various carbohydrate heads (*β*-D-*gluco*, *β*-D-*galacto*, *β*-*lacto*, *β*-D-*xylo*, and α-D-*manno*) have been synthesized. The key step was the formation of phenyldiazonium tetrafluoroborates **2a**−**e** from the per-*O*-acetylated 4-aminophenyl glycosides **1a**−**e**. These salts were condensed with *N*,*N*-didodecylaniline under phase transfer conditions and the per-*O*-acetylated 4-(4′-*N*,*N*-didodecylaminophenylazo)phenyl 1,2-trans glycosides **4a**−**e** were fully de-*O*-acetylated by the Zemplén method. The self-organizing liquid crystal properties of the compounds were investigated by a variety of techniques, including polarized light microscopy, differential scanning calorimetry, and X-ray diffraction. All but one of the materials exhibited smectic A, lamellar phases. Remarkably, the glucose derivative exhibited a rectangular disordered columnar phase. This result has implications with respect to the induced curvature created by the recognition processes of the glucose headgroup relative to the other sugar moieties and to the prevalence of various glycolipids in cell membranes

## 1. Introduction

Many biological processes are mediated by recognition events involving complex carbohydrates, mostly by interactions between proteins and the carbohydrate moiety of glycoconjugates (glycolipids, glycopeptides). In the interaction phenomenon, the terminal carbohydrate headgroup is generally responsible for the binding with the protein receptor.[1−4] Since glycolipids are basic constituents of biological membranes, we have recently synthesized several neoglycolipids to understand their self-organizing properties with regard to their structures. The latter possessed a carbohydrate head (*N*-acetyl-D-glucosamine, D-galactose) and hydrophobic chains either directly attached together in the case of neoglycosyl ceramides analogues[5,6] or linked either by an oligoethyleneglycol[7,8] or an alditol[9] spacer. Some of these compounds displayed both thermotropic and lyotropic liquid crystal properties.[6] Furthermore, the carbohydrate head has the potential to be used as a recognition signal toward lectins in supramolecular assemblies such as monolayers[5,7,10] or liposomes.[11] This paper deals with the synthesis of a new class of neoglycolipids in which the spacer between the sugar and the lipid moiety is a phenylazophenyl group endowed with UV−visible light adsorption properties.

Phenylazophenyl glycosides and related derivatives are well-known because they have been found to have a large variety of applications, for example, as probes for the activity of a polysaccharide α-amylase,[12] inhibitors of cell growth,[13] dyes for polyester fibers,[14] and very recently, as gelators.[15] Nevertheless, to our knowledge, none of these compounds possess hydrophobic moieties capable of inducing self-organizing properties.

Conversely, azobenzene-based materials have been used for a number of years in liquid crystal systems for investigations into optical and thermally addressed read−write data storage systems and in surface command structures. By controlling the interconversion of cis to trans isomers, it has been possible to control the nematic liquid crystal to isotropic liquid phase transition and, thus, to design material systems which can be

[†] Université Lyon 1.
[§] The University of Hull.

(1) Varki, A. *Glycobiology* **1993**, *3*, 97−130.
(2) Dwek, R. A. *Chem. Rev.* **1996**, *96*, 683−720.
(3) Lis, H.; Sharon N. *Chem. Rev.* **1998**, *98*, 637−674.
(4) Evans, S. V.; MacKenzie, C. R. *J. Mol. Recognit.* **1999**, *12*, 155−168.
(5) Lafont, D.; Bouchu, M.-N.; Girard-Egrot, A.; Boullanger, P. *Carbohydr. Res.* **2001**, *336*, 181−194.
(6) Dumoulin, F.; Lafont, D.; Boullanger, P.; Mackenzie, G.; Mehl, G. H.; Goodby, J. W. *J. Am. Chem. Soc.* **2002**, *124*, 13737−13748.
(7) Boullanger, P.; Sancho-Camborieux, M.-R.; Bouchu, M.-N.; Marron-Brignone, L.; Morelis, R. M.; Coulet, P. R. *Chem. Phys. Lipids* **1997**, *90*, 63−74.
(8) Lafont, D.; Boullanger, P.; Chierici, S.; Gelhausen M.; Roux, B. *New J. Chem.* **1996**, *20*, 1093−1101.
(9) Lafont, D.; Gross, B.; Kleinegesse, R.; Dumoulin, F.; Boullanger, P. *Carbohydr. Res.* **2001**, *331*, 107−117.
(10) Berthelot, L.; Rosilio, V.; Costa, M. L.; Chierici, S.; Albrecht, G.; Boullanger, P.; Baszkin A. *Colloids Surf., B* **1998**, *11*, 239−248.
(11) Gelhausen, M.; Besson, F.; Chierici, S.; Lafont, D.; Boullanger, P.; Roux, B. *Colloids Surf., B* **1998**, *10*, 395−404.
(12) Osada, C. Eur. Pat. Appl., EP 298,516 (Cl. C07/H15/203) Jan 11, 1989; JP Appl., 87/170499, July 8, 1987; 20 pp; *Chem. Abstr.* **1989**, *111*, 58265.
(13) Serpe, M. D.; Nothnagel, E. A. *Planta* **1994**, *193*, 542−550.
(14) Arias, M. J. L.; Girardi, E.; Navarro, J. A.; Savarino, P.; Valldeperas, J.; Viscardi, G. *Dyes Pigm.* **2000**, *46*, 37−42.
(15) Amaike, M.; Kobayashi, H.; Shinkai, S. *Chem. Lett.* **2001**, 620−621.

10.1021/ja037347x CCC: $25.00 

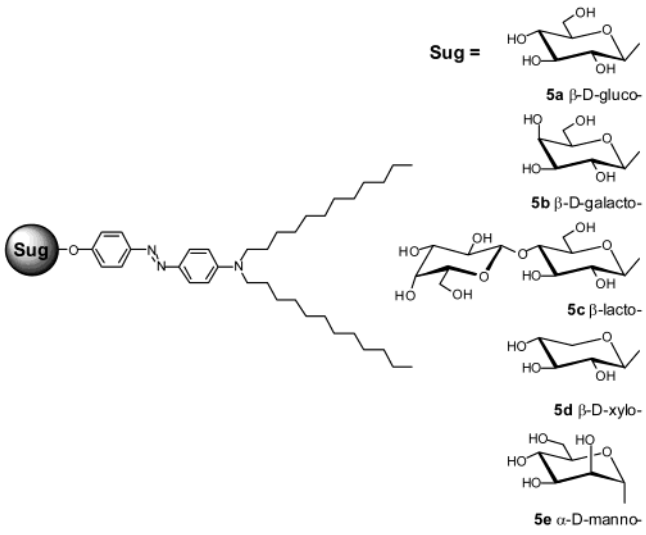


***Figure 1.*** Structural design and target materials.

switched from the optically isotropic liquid phase to the optically anisotropic mesomorphic state.[16−18]

Thus, it was our objective in this study to combine the responsiveness provided by the azobenzene motif with the self-organizing properties of amphiphilic materials relevant to biological systems. Our initial studies in this area, which we report here, concern the characterization of the mesophases formed by a family of analogous materials, selected with the aim of permitting a systematic study to establish property structure−activity relationships.

The materials selected, **5a**−**e**, were designed to have two dodecyl terminal chains similar to those found in biological membranes, an azobenzene unit which would be responsive to optical and thermal stimuli, and a sugar moiety which would act as a hydrophilic, microphase-segregating, and biocompatible group (Figure 1). Within the series **5a**−**e**, the sole variation was the sugar moiety.

**2. Synthetic Strategy.** Two routes have been reported in the literature for the synthesis of phenylazophenyl glycosides. In the first, a phenylazophenol derivative was directly glycosylated using either peracetylated glycopyranoses or glycopyranosyl halides, generally affording 1,2-*trans*-glycosides in moderate yields.[12,19−21] In the second, the starting material was a 4-aminophenyl glycoside, which was diazotized by standard methods and reacted in situ with an aromatic compound.[22−24] The better yields generally obtained by the second approach prompted us to use it for our syntheses. The starting materials were per-*O*-acetylated 4-aminophenyl $\beta$-D-glycopyranosides **1a**−**d**[25−28] (**a**: $\beta$-D-*gluco*, **b**: $\beta$-D-*galacto*, **c**: $\beta$-*lacto*, **d**: $\beta$-D-*xylo*), which were synthesized in two steps from the corresponding peracetylated glycosyl bromides. Thus, the 4-nitrophenyl $\beta$-D-glycopyranosides were obtained according to the method of Kleine et al.[26] and then reduced by hydrogen transfer.[27] Compound **1e**[29] (**e**: $\alpha$-D-*manno*) was prepared by fusion of 1,2,3,4,6-penta-*O*-acetyl-$\beta$-D-mannopyranose and 4-nitrophenol in the presence of zinc chloride,[30] followed by reduction of the 4-nitrophenyl glycoside by hydrogen transfer.

***Scheme 1*** [a]

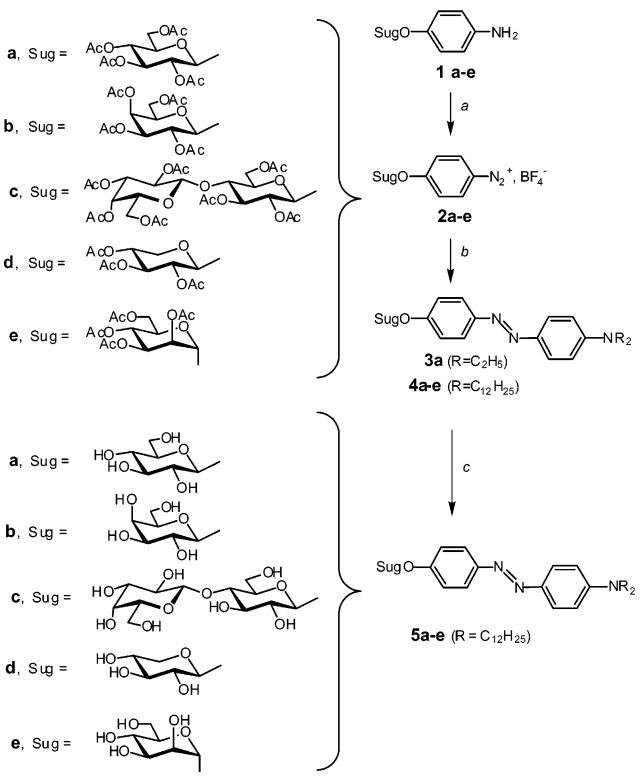


[a] a: $BF_3{\cdot}OEt_2$ (1.5 equiv), −15 °C, **1a**−**e**, 15 min, then *t*-$BuNO_2$, −15 to 0 °C. b: **2a**−**e**, picric acid (cat), $R_2NC_6H_5$ (1.2 equiv), $Na_2CO_3$, $(ClCH_2)_2$, $H_2O$. c: **4a**−**e**, NaOMe (cat), MeOH.

The preparation of the phenylazophenyl glycosides is depicted in Scheme 1. Numerous methods are described in the literature for the synthesis of aryldiazonium salts from aniline derivatives.[31] The salts most commonly used are chlorides, trifluoroacetates, and tetrafluoroborates. Aryldiazonium trifluoroacetates are more soluble in organic solvents than their tetrafluoroborate counterparts but have the disadvantage of being less stable.[32] In addition, tetrafluoroborates possess a greater stability than the corresponding chlorides and have the advantage of being prepared easily in anhydrous media from aromatic amines. Therefore, aryldiazonium tetrafluoroborates were chosen for the present study. Application of the method described by Doyle et al.[33] to the peracetylated 4-aminophenyl glycosides **1a**−**e** (*t*-BuONO, $BF_3{\cdot}OEt_2$, −15 °C, $CH_2Cl_2$) gave the expected tetrafluoroborates **2a**−**e** sufficiently pure for the next step. The

(16) Pelzl, G. *Z. Chem.* **1977**, *17*, 294−295.
(17) Ikeda, T.; Miyamoto, T.; Kurihara S.; Tazuke, S. *Mol. Cryst. Liq. Cryst.* **1990**, *188*, 207−222.
(18) Legge, C. H.; Mitchell, G. R. *J. Phys. D: Appl. Phys.* **1992**, *25*, 492−499.
(19) Hurd, C. D.; Bonner, W. A. *J. Org. Chem.* **1946**, *11*, 50−54.
(20) Hurd, C. D.; Zelinski, R. P. *J. Am. Chem. Soc.* **1947**, *69*, 243−246.
(21) Hiroshi, S. Jpn. Kokai Tokkyo Koho, JP 02 83,391 (Cl. C07 H15/203), March 23, 1990, Appl., 88/235,964, Sept 20, 1988; 13 pp; *Chem. Abstr.* **1990**, *113*, 132695*s*.
(22) Ganjian, I.; Basile, D. V. *Anal. Biochem.* **1997**, *264*, 252−255.
(23) Barni, E.; Barolo, C.; Quagliotto, P.; Valldeperas, J.; Viscardi, G. *Dyes Pigm.* **2000**, *46*, 29−36.
(24) Amaike, M.; Kobayashi, H.; Sakurai, K.; Shinkai, S. *Supramol. Chem.* **2002**, *14*, 245−253.
(25) Ram, S.; Ehrenkaufer, R. E. *Tetrahedron Lett.* **1984**, *25*, 3415−3418.
(26) Kleine, H. P.; Weinberg, D.; Kaufmann, R. J.; Sidhu, R. S. *Carbohydr. Res.* **1982**, *142*, 333−337.
(27) Roy, R.; Tropper, F. D.; Morisson, T.; Boratynski, J. *J. Chem. Soc., Chem. Commun.* **1991**, 536−538.
(28) De Bruyne, C. K.; Van Wijnendaele, F. *Carbohydr. Res.* **1967**, *4*, 101−103.
(29) Page, D.; Zanini, D.; Roy, R. *Bioorg. Med. Chem.* **1996**, *4*, 1949−1961.
(30) Conchie, J.; Levy, A. *Methods Carbohydr. Chem.* **1962**, *2*, 345−347.
(31) Schank, K. In *The Chemistry of Functional Groups: The Chemistry of Diazonium and Diazo Groups*; Pataï, S., Ed.; John Wiley & Sons: New York, 1978; Vol. 2, pp 645−658.
(32) Colas, C.; Goeldner, M. *Eur. J. Org. Chem.* **1999**, 1357−1366.
(33) Doyle, M. P.; Bryker, W. J. *J. Org. Chem.* **1979**, *44*, 1572−1574.

NMR data ($^1$H and $^{13}$C) recorded for the salts **2a**−**e** were in agreement with those of the literature,[32−34] and the structure of compound **2b** was furthermore confirmed by determination of its exact mass. The azo coupling reaction was first investigated using *N*,*N*-diethylaniline[35] and the tetrafluoroborate **2a** under phase transfer conditions catalyzed by picrate ions, according to the methodology described by Hashida et al.[36] These authors suggested that the higher reactivity of the diazonium salts with the picrate counterion could be ascribed to weaker ion pairing, thus increasing the electrophilicity of the diazonium ion. Therefore, our reaction was performed in a 1,2-dichloroethane and water mixture in the presence of sodium carbonate and a catalytic amount of picric acid. The expected phenylazophenyl derivative **3a** was obtained in 43% yield after purification. Better yields (55−72%) were obtained for the preparation of the phenylazophenyl derivatives **4a**−**e** from **2a**−**e** and *N*,*N*-didodecylaniline[37] using similar conditions. The structures of the compounds **3a** and **4a**−**e** were ascertained from $^1$H and $^{13}$C NMR spectra by comparison with the literature data.[23,38−40] The fully deprotected derivatives **5a**−**e** were obtained by de-*O*-acetylation under Zemplén conditions.

## 3. Results

In the following sections, the mesophase properties and self-organized structures formed by compounds **5a**−**e** are described. Their properties were investigated by thermal polarized light optical microscopy (POM), differential scanning calorimetry (DSC) relative to indium standards,[41] and X-ray diffraction. Details of the experimental techniques used can be found in the Supporting Information.

**3.1. 4-(4′-*N*,*N*-Didodecylaminophenylazo)phenyl β-D-Glucopyranoside (5a).** Upon heating a pristine sample of compound **5a**, we could observe no melting point by transmitted polarized light microscopy. This was due to the fact that the material was highly colored, and paramorphosis at a potential melting point would not allow us to observe a phase transition, i.e., there were a large number of defects leading to small domains in the pristine sample which made it difficult to observe any changes on heating. As the temperature was raised to over 150 °C, a typical liquid crystalline texture was observed as the material became more fluid. At 181.2 °C, the material melted to give the amorphous liquid. Cooling of the sample resulted in a transition back to the liquid crystal state. The transition temperature of 175.6 °C was slightly lower because of decomposition of the sample. No further changes in defect texture of the mesophase were obtained upon cooling of the material down to room temperature. Mechanical shearing of the specimen showed that the compound had undergone glassification.

The defect texture exhibited by compound **5a** is shown in Figure 2. It can be seen from the photomicrograph that the material is red in color, making the defects difficult to see. Nevertheless, the texture has a fanlike appearance, and close observation shows that although there are large numbers of fanlike defects, none possess hyperbolic and elliptical lines of optical discontinuity associated with focal−conic defects and smectic phases. Therefore, although the photomicrograph has the appearance of a smectic phase, it is clearly not lamellar. Thus, the indications are that the phase is columnar. The absence of concentric defect lines across the fanlike regions, which are associated with long-range translational ordering, indicates that the columnar structure of the phase is disordered along the column axes. Initial observations also suggest that the phase possibly has an hexagonal arrangement of columns. Thus, the initial classification of the phase from textural studies would be a disordered columnar phase, with possibly an hexagonal arrangement of the columns, i.e., $Col_{hd}$. X-ray diffraction was employed (discussed later) to investigate this initial classification in more detail.

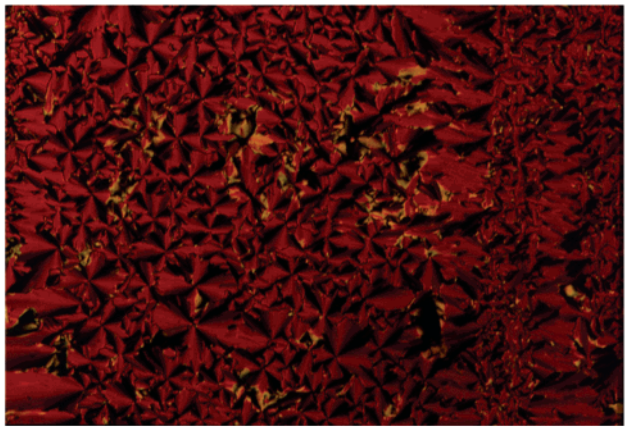

***Figure 2.*** Defect texture of compound **5a** formed upon cooling from the isotropic liquid (×100).

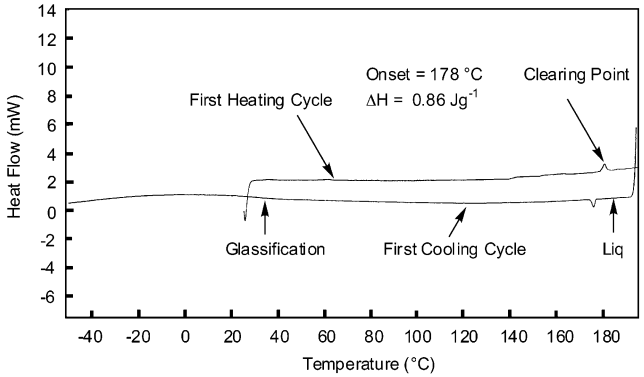


***Figure 3.*** DSC traces, heating and cooling, for compound **5a**, scanning rate 10 °C min$^{-1}$.

Differential scanning calorimetry confirmed the results obtained from POM (Figure 3). Upon heating a pristine sample, the material appeared to be in its mesomorphic state at or near room temperature. At 179 °C ($\Delta H = 0.86$ Jg$^{-1}$), the material melted from the liquid crystal state to the isotropic liquid. No other phase transitions were observed showing that compound **5a** only exhibits one mesophase. Upon cooling, the clearing point occurred at approximately five degrees lower, indicating that the material had undergone slight decomposition in the liquid state. As it cooled to room temperature, compound **5a** underwent a glass transition at approximately 25 °C. It is also

(34) Korzeniowski, S. H.; Leopold, A.; Beadle, J. R.; Ahern, M. F.; Sheppard, W. A.; Khanna, R. J.; Gokel, G. W. *J. Org. Chem.* **1981**, *46*, 2153−2159.
(35) Srivastava, S. K.; Chauhan, P. M. S.; Bhaduri, A. P. *Synth. Commun.* **1999**, *29*, 2085−2092.
(36) Hashida, Y.; Kubota, K.; Sekiguchi, S. *Bull. Chem. Soc. Jpn.* **1988**, *61*, 905−909.
(37) Liang, K.; Law, K.-Y.; Whitten, D.-G. *J. Phys. Chem. B* **1997**, *101*, 540−546.
(38) Savarino, P.; Viscardi, G.; Barni, E.; Carpignano, R.; Fedorov, L. A. *Dyes Pigm.* **1990**, *13*, 71−80.
(39) Fedorov, L. A.; Savarino, P.; Dostovalova, V. I.; Viscardi, G.; Carpignano, R.; Barni, E. *Magn. Reson. Chem.* **1991**, *29*, 747−748.
(40) Simova, S.; Radeglia, R.; Ganghänel, E. *J. Prakt. Chem.* **1982**, 777−786.
(41) *CRC Handbook of Physics and Chemistry*, 68th ed.; Priest, R. C., Ed.; CRC Press: Boca Raton, FL, 1988.

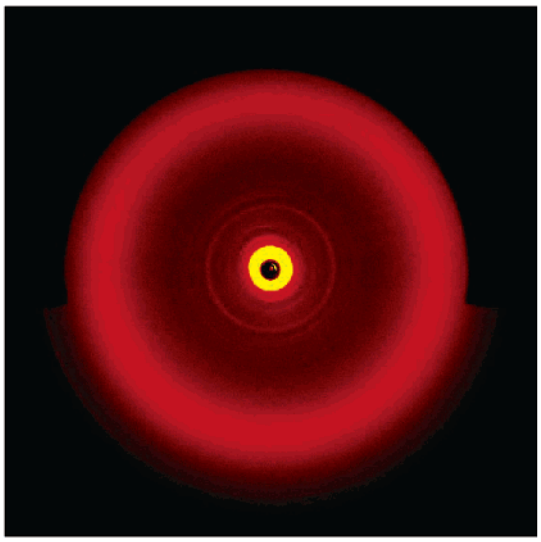

***Figure 4.*** Powder diffraction pattern for compound **5a** at 30 °C. The maximum diffraction angle was $2\theta = 30°$.

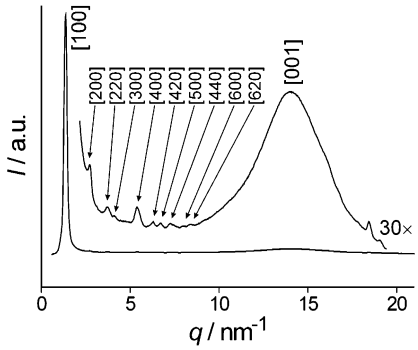


***Figure 5.*** Radially integrated diffraction pattern of compound **5a** at 30 °C.

interesting to note that the enthalpy of the phase transition from the liquid crystal phase to the isotropic liquid is relatively small, indicating that the mesophase is disordered and liquidlike.

X-ray diffraction studies of **5a** were performed across a wide temperature range in the mesophase of the material. The diffractogram, taken at 30 °C and displayed in Figure 4, shows a typical example. The radially integrated diffraction pattern of compound **5a** at 30 °C is shown in Figure 5, where for clarity, the wide-angle region has been magnified 30 times. Table 1 shows the distances (Å) related to the Miller indices shown in the graph in Figure 5.

The calculated spacings, shown in Table 1, were obtained after fitting the experimentally observed spacings to a monoclinic unit cell, where the best fit for the data was obtained for a nearly rectangular cell of dimensions $a = b = 46.5$ Å and $\alpha = 90.5°$. Thus, the glucose derivative **5a** shows the X-ray characteristics of a columnar rectangular cell. The lateral reflections were indexed up to the [620] reflection, indicating a high extent of columnar ordering. However, the intracolumnar order of the mesogenic moieties and aliphatic chains is low, as shown by the diffuse reflection at 4.5 Å. At wide angles, two more (sharp) reflections are observed (with spacings of 3.41 and 3.30 Å), which can be attributed to well-organized sugar headgroups. Thus, the columnar structure has well-organized carbohydrate moieties at the cores of the columns, whereas the mesogenic cores are relatively disordered and the aliphatic chains are "melted". Therefore, the mesophase is classified as $Col_r$.

***Table 1.*** Distances (Å) Related to the Miller Indices Shown in the Graph in Figure 5 for the Radially Integrated Diffraction Pattern of Compound **5a** at 30 °C

| Miller indices | $q_{exp}$/nm$^{-1}$ | $d_{exp}$/Å | $d_{calc}$/Å |
|---|---|---|---|
| [100] | 1.36 | 46.3 | 46.5 |
| [200] | 2.72 | 23.2 | 23.3 |
| [220] | 3.70 | 16.9 | 16.7 |
| [300] | 4.09 | 15.4 | 15.5 |
| [400] | 5.38 | 11.7 | 11.6 |
| [420] | 6.28 | 10.1 | 10.5 |
| [500] | 6.7 | 9.3 | 9.3 |
| [440] | 7.3 | 8.7 | 8.4 |
| [600] | 8.0 | 7.8 | 7.8 |
| [620] | 8.4 | 7.3 | 7.4 |
| [001] | 14.1 | 4.5 | |

The molecular length of the glucose derivative **5a** was determined by two different methods. Dreiding molecular models gave the molecular length as approximately 32 Å, whereas minimized structures from computer simulations using ChemDraw 3D gave the molecular length as 32.3 Å. The two measurements were in approximate agreement, thus giving the average molecular length as 32 ± 1 Å. This result indicates that the molecules must appreciably overlap between the columns in the mesophase, which are approximately 46.5 Å apart. For a molecular length of 32 Å, twice the molecular length of 64 Å results in an overlap, or interpenetration, of at least 8.75 Å.

**3.2. 4-(4′-*N*,*N*-Didodecylaminophenylazo)phenyl β-D-Galactopyranoside (5b).** On heating the galactose derivative **5b**, no melting point was observed by POM due to the material being colored and paramorphosis occuring at a potential melting point. As the temperature was raised to near the clearing point, a typical liquid crystalline texture was observed as the material became more fluid. At 184 °C, the material melted to give the amorphous liquid. Cooling of the sample resulted in a transition back to the liquid crystal state at approximately 179 °C. As with **5a**, the transition temperature was slightly lower than the one obtained on heating because of decomposition of the sample. No further changes in defect texture of the mesophase was obtained upon cooling of the material down to room temperature. Mechanical shearing of the specimen showed that the compound had undergone glassification near to room temperature.

The defect texture exhibited by the liquid crystal phase is shown in Figure 6. It can be seen, in comparison with Figure 2, that the microscopic texture of **5b** is appreciably different from **5a**. Most of the texture appears to be in a focal−conic state; however, there are no elliptical and hyperbolic lines of optical discontinuity to confirm this observation, except for one such defect located near the top of the photomicrograph in Figure 6 (see black cross to the left of the white arrow). The presence of this defect strongly suggests that this phase is not columnar, but lamellar. It should also be noted that the black areas in the texture are not homeotropic but are instead due to air bubbles. Thus, we do not have the luxury of being able to confirm the classification of the phase as being lamellar through the presence of both focal−conic and homeotropic textures.

Differential scanning calorimetry confirmed the transition temperatures obtained from POM (Figure 7). Slight differences

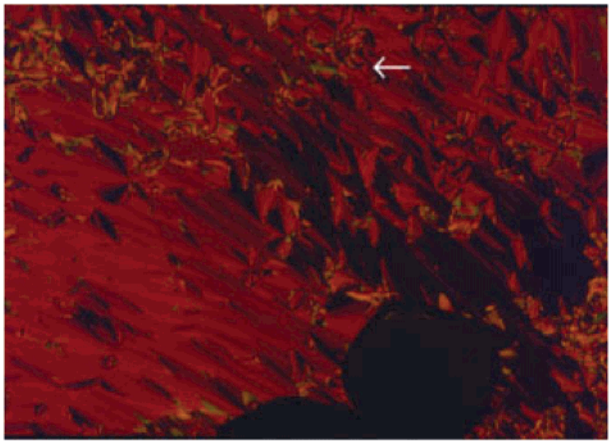

***Figure 6.*** Defect texture of compound **5b** formed upon cooling from the isotropic liquid (×100). To the left of the arrow there is an elliptical/hyperbolic disclination.

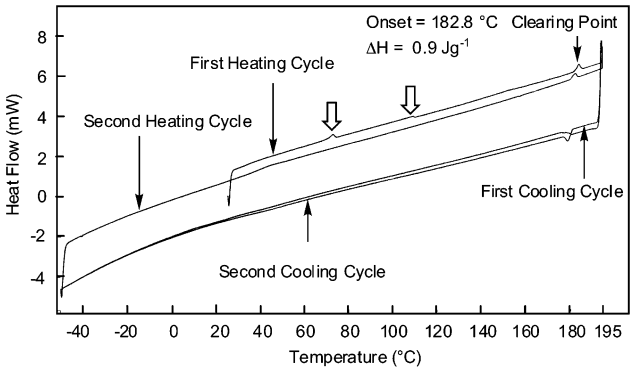


***Figure 7.*** DSC traces, heating and cooling, for compound **5b**, scanning rate 10 °C $min^{-1}$.

in temperatures with respect to POM were due to different rates of decomposition in aluminum pans versus glass slides. Heating a pristine sample resulted in the material appearing to melt at 70.4 °C ($\Delta H = 0.96$ $Jg^{-1}$). However, the enthalpy for this transition was very low, which made us consider if another mesophase was present, but on cooling no thermal event occurred at, or near to, this temperature, thus demonstrating that the transition is not one between two mesophases. At 182.8 °C ($\Delta H = 0.9$ $Jg^{-1}$), compound **5b** melted from the liquid crystal state to the isotropic liquid. An anomaly in the DSC baseline was also observed at approximately 110 °C (marked by an open arrow in Figure 7), but this was not reproducible in further heating and cooling cycles. As no other phase transitions were observed upon subsequent heating and cooling, we can conclude that compound **5b** only exhibits one mesophase.

In the cooling cycles of the material, the clearing point occurred a few degrees lower than observed in the first heating cycle, indicating that the material had undergone slight decomposition in the liquid state. As it cooled to room temperature under POM, compound **5b** appeared to glassify; however, no glass transition was detected by DSC, thus indicating that the kinetic process was very slow. It is also interesting to note that the enthalpy of the phase transition from the liquid crystal phase to the isotropic liquid is relatively small and almost identical to that for **5a**, indicating that the mesophase is disordered and liquidlike.

Powder X-ray diffraction investigations of the galactose derivative **5b** were performed across a wide temperature range

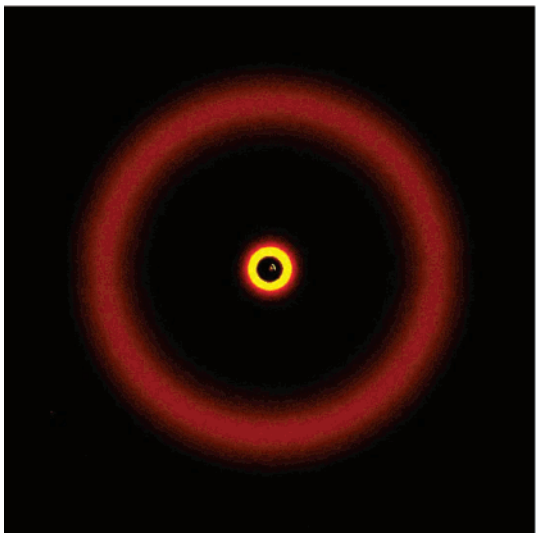

***Figure 8.*** Powder diffraction pattern for the galactose derivative **5b** at 90 °C. The maximum diffraction angle was $2\theta = 30°$.

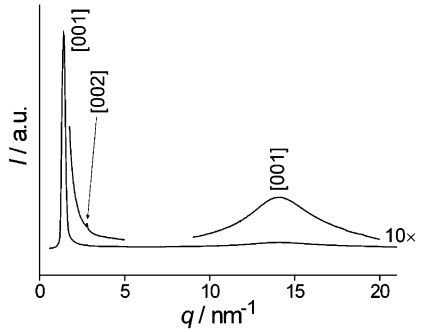


***Figure 9.*** Radially integrated diffraction pattern of compound **5b** at 90 °C

***Table 2.*** Distances (Å) Related to the Miller Indices Shown in the Graph in Figure 9 for the Radially Integrated Diffraction Pattern of Compound **5b** at 90 °C

| Miller indices | $q$/nm$^{-1}$ | $d$/Å |
|---|---|---|
| [001] | 1.41 | 44.6 |
| [002] | 2.85 | 22.1 |
| [100] | 14.2 | 4.4 |

in the mesophase of the material. Typical powder diffraction results for the material, shown in Figure 8, were taken at 90 °C. The radially integrated diffraction pattern of **5b** at 90 °C is shown in Figure 9, and Table 2 shows the distances (Å) related to the Miller indices shown in the graph in Figure 9. For clarity, the wide-angle region and the [002] reflection have been magnified 10 times.

Thus, the X-ray diffraction patterns of the galactose compound **5b** are characteristic of smectic A types of mesophase, i.e., a strong principal [001] reflection of the smectic layers, and a weak second-order [002] reflection, combined with a diffuse intermolecular [100] reflection.

The molecular length of the galactose derivative **5b** was determined to be approximately 30 Å by Dreiding molecular models and 30.859 Å from computer simulations using ChemDraw 3D. The two measurements were in approximate agreement, giving the average molecular length as 30 ± 1 Å. This result indicates that in the lamellar phase of **5b** the molecules must appreciably overlap between the layers in the mesophase, thereby giving a structure with a bilayer ordering which has a

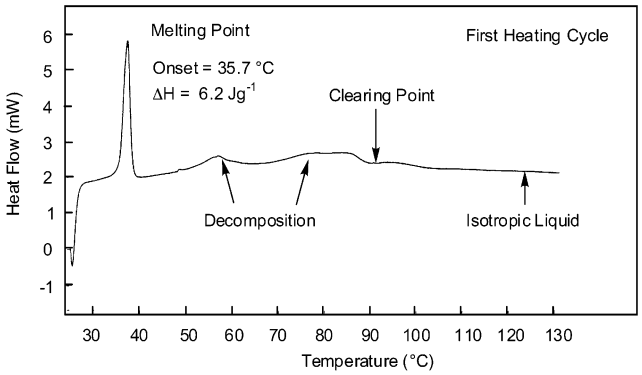


***Figure 10.*** DSC traces, heating and cooling, for compound **5e**, scanning rate 10 °C min$^{-1}$.

repeat of approximately 44.6 Å. For a molecular length of 30 Å, this means that molecules overlap, or interpenetrate, between layers by approximately 7.7 Å.

**3.3. 4-(4′-*N,N*-Didodecylaminophenylazo)phenyl 4-*O*-*β*-D-Galactopyranosyl-*β*-D-glucopyranoside (5c).** The lactose compound, **5c**, was found to exhibit mesomorphic properties by polarizing light microscopy. The material was found to melt at 139 °C upon heating and to have an isotropization point at 266 °C, but at this temperature it starts to decompose or undergo isomerization rapidly. In fact, the material started to decompose or isomerize as soon as the liquid crystal state was formed. The decomposition/isomerization process made it difficult to obtain meaningful data on this material. For example, DSC showed no thermal events at all, and the baseline showed considerable nonlinearity as the temperature was changed. As a consequence, X-ray diffraction studies were not undertaken.

Thus, mesophase classification relied on thermal polarized light microscopy. The material exhibited textures similar to those obtained for the smectic A phase. However, without X-ray diffraction studies it is difficult to make a firm classification. Upon addition of water to investigate the lyotropic phases of the material, lamellar phases were unequivocally obtained.

**3.4. 4-(4′-*N,N*-Didodecylaminophenylazo)phenyl *β*-D-Xylopyranoside (5d).** The xylose derivative **5d** was, surprisingly, found not to exhibit mesomorphism. Upon being heated, the material simply melted at 120−122 °C to give an amorphous liquid. No defect textures were observed that could be associated with liquid crystal phases. Similarly, the DSC showed no phase transitions other than melting to the liquid phase. As no mesophase transitions were observed, the material was not investigated further by other methods such as X-ray diffraction.

**3.5. 4-(4′-*N,N*-Didodecylaminophenylazo)phenyl α-D-Mannopyranoside (5e).** The mannose derivative, **5e**, behaved much the same as the galactose derivative, **5b**, in POM studies, except that it apparently melted to a liquid at a temperature of approximately 90 °C. It appeared that some decomposition occurred with this process. The textures observed were not as well-developed as those obtained for **5b**. Typically small domains were obtained, and because of the color of the material, transmission through the specimens was poor. Nevertheless, the textures obtained were similar to those found for the smectic phase of **5b**.

DSC confirmed the results obtained from POM. The material melted at 35.7 °C ($\Delta H$ = 6.9 Jg$^{-1}$), and upon further heating the baseline became unstable, indicating that the material was undergoing some decomposition. The clearing point of approximately 90 °C obtained via POM was not detected as a thermal event in DSC. After this point, the baseline became flat and up to a temperature of 145 °C no more peaks were observed (Figure 10). Cooling produced a DCS with no peaks at all, indicating that decomposition or *cis*−*trans* isomerization of the azo-linkage may have taken place once the liquid state had been achieved. Indeed, the formation of the *cis*-isomer would be detrimental to the stability of the lamellar phase as the material would have an overall bent molecular shape rather than a rodlike shape.

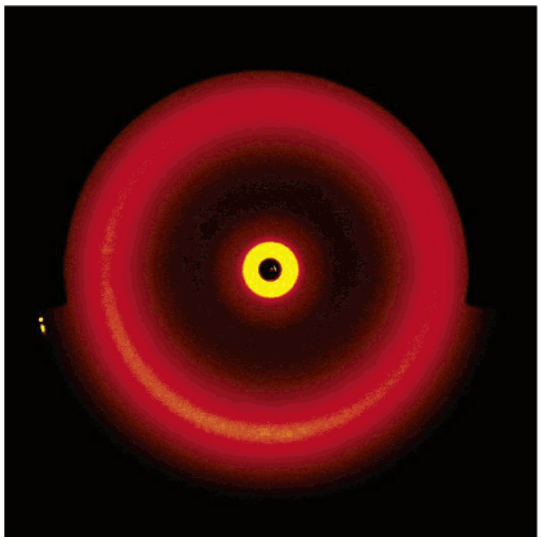

***Figure 11.*** Powder diffraction pattern for mannose derivative **5e** at 75 °C. The maximum diffraction angle was $2\theta = 30°$.

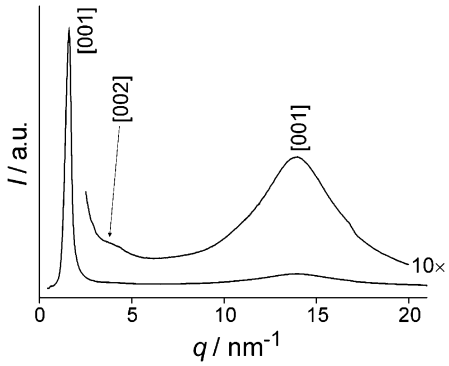


***Figure 12.*** Radially integrated diffraction pattern of compound **5e** at 75 °C.

***Table 3.*** Distances (Å) Related to the Miller Indices Shown in the Graph in Figure 12 for the Radially Integrated Diffraction Pattern of Compound **5e** at 75 °C

| Miller indices | *q*/nm$^{-1}$ | *d*/Å |
|---|---|---|
| [001] | 1.60 | 39.3 |
| [002] | 3.26 | 19.3 |
| [001] | 13.8 | 4.5 |

X-ray diffraction investigations on the mannose derivative **5e** were performed at 75 °C in the mesophase of the material. A typical powder diffraction pattern for the material is shown in Figure 11. The radially integrated diffraction pattern of **5e** at 75 °C is shown in Figure 12, and Table 3 shows the distances (Å) related to the Miller indices. The diffraction patterns of the mannose derivative **5e** are thus characteristic of a smectic A

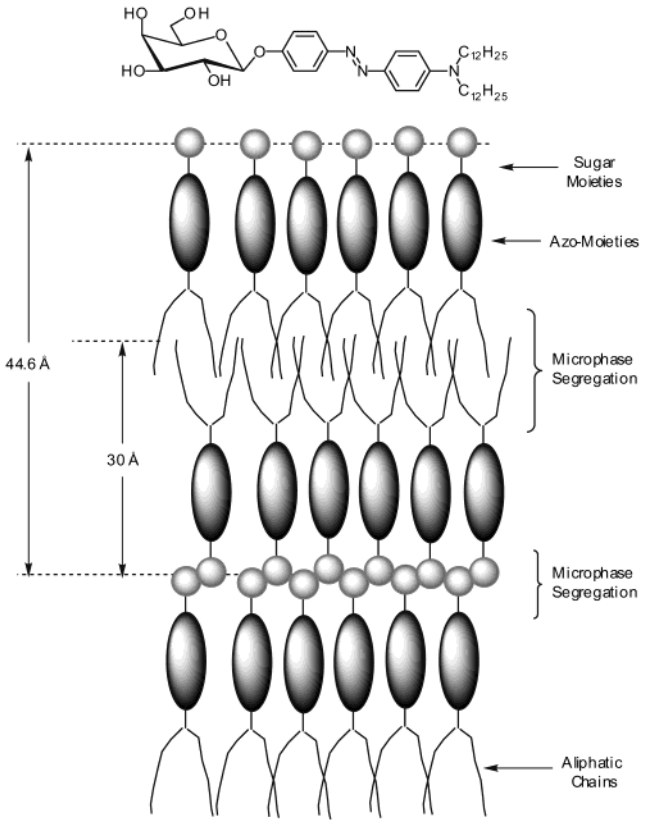


***Figure 13.*** Interdigitated smectic $A_d$ structure of the galactose derivative **5b**.

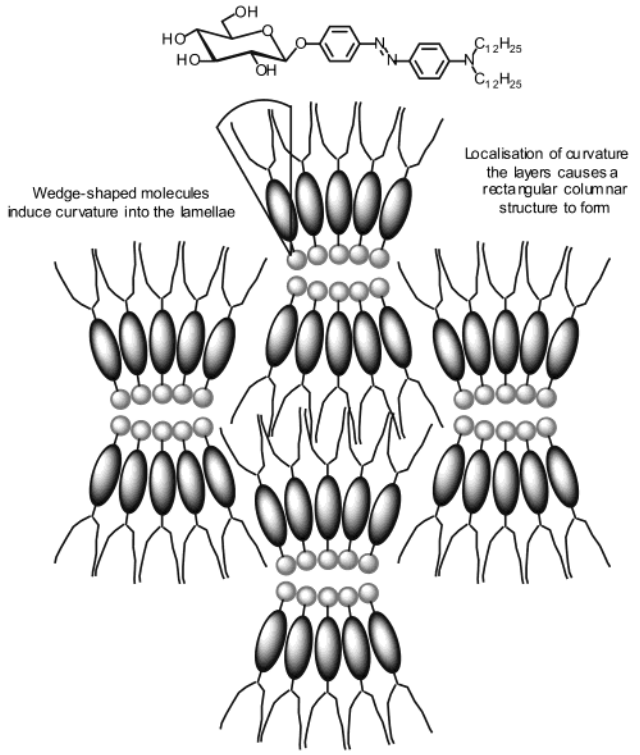


***Figure 14.*** Formation of a columnar structure in the lamellar phase due to the introduction of curvature into the system.

mesophase, with a strong principal [001] reflection and a weak second-order [002] reflection associated with the smectic layers.

## 4. Discussion

The results obtained from POM, DSC, and XRD show that the galactose, lactose, and mannose derivatives (**5b**,**c**,**e**) exhibit interdigitated smectic $A_d$ phases, with a layer spacing $d = 1.48 \times l$ where $l$ is the molecular length. Therefore, it is reasonable to assume that the structure is microphase-segregated, i.e., the carbohydrate moieties of the individual molecules tend to congregate together, as do the aliphatic chains. It is also reasonable to assume that there will be half-layer shifts in the structure of the phase at walls and defects. Thus, the structure of the mesophase does not consist of continuous sandwiches of aliphatic regions and carbohydrate layers. Furthermore, as the molecules have two aliphatic chains it is likely that there will be curvature introduced into the system at the layer interfaces between the chains because the cross-sectional area of two aliphatic chains is larger than a carbohydrate moiety. The curvature could possibly be minimized by the formation of an in-plane modulation, as found in smectic $\tilde{A}$ phases. Such an in-plane modulation may serve as the nucleation point in the formation of a columnar structure as described later. At the interfaces between the carbohydrate moieties, the sugar units will hydrogen-bond, but in a dynamic fashion. Indeed, the sugars may even interdigitate between layers. Thus, an average picture of the mesophase structure is represented in Figure 13 for compound **5b**.

The glucose derivative **5a** was shown to exhibit a rectangular columnar disordered mesophase, $Col_r$, and thus it is interesting to speculate why this result is found when the galactose analogue exhibits a lamellar phase. The molecular structures of all of the materials prepared have gross wedgelike shapes. The two aliphatic tails will be liquidlike in their mesophases and therefore will occupy a larger cross-sectional area with respect to the aromatic and sugar moieties of the molecules. The packing of wedgelike molecules in a microphase-segregated system inevitably means that curvature will be introduced into the layers. When the curvature reaches a critical point the layers will break up, and there is a potential for columns to be formed as shown in Figure 14. The half-layer shifts in the structure will form the nucleation points for the introduction of a columnar structure. Thus, the transition to the columnar phase might proceed through the formation of an intermediary smectic $\tilde{A}$ phase which has an in-plane modulation. However, this phase would also be expected to be transitory and therefore difficult to observe by X-ray diffraction.

Overall, we can propose a structure for the rectangular columnar phase as shown in Figure 15. Although the columns in the figure are drawn in a discrete way, it should be remembered that the aliphatic tails of the molecules will interpenetrate from one column to the next such that the centers of the columns will possess carbohydrate moieties saturated in a lipid sea.

Why the glucose derivative should exhibit a columnar phase whereas the galactose, mannose, and lactose derivatives exhibit lamellar phases is an interesting question. For the galactose and mannose derivatives **5b**,**e**, each has an axial hydroxyl group, whereas glucose contains all equatorial hydroxyl groups. Thus, the recognition/packing of the glucose moieties is expected to be closer than for the corresponding sugars, thereby accentuating the wedgelike shape of the molecular structure. It may be therefore that the curvature imparted by the glucose moiety tips the balance from lamellar to columnar. This presupposes that

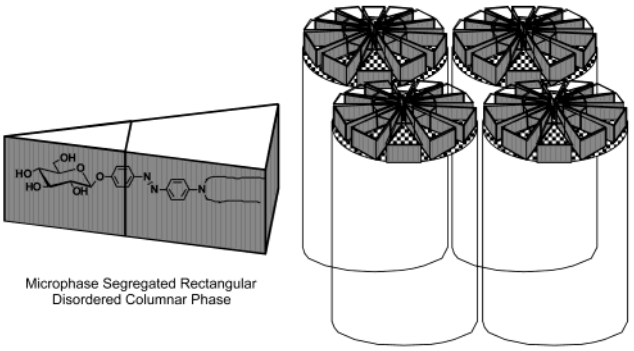


***Figure 15.*** Disordered rectangular columnar structure of the glucose derivative **5a**. Although the columns in the figure are drawn in a discrete way, it should be remembered that the aliphatic tails of the molecules will interpenetrate from one column to the next.

the other sugar systems are very close to becoming columnar themselves, which is probably why their microscopic textures are so similar to those of columnar phases. The lactose derivative is much longer than the galactose or mannose materials and therefore will have much less of a wedge-shaped molecular structure. Therefore, the induced curvature will be less such that the material might be expected to exhibit stronger lamellar phase properties than the monosaccharides **5b**,**e**. In addition, the length of the lactose unit and the larger number of free hydroxyl groups means that this material will have a much higher clearing point in comparison to the monosaccharide systems. Hence, the clearing point is higher than 200 °C, and at such temperatures decomposition becomes problematical in the characterization of mesophase structures.

This result may, therefore, have some relevance to the relative abundance of glycolipids in biological membranes. It appears that glucose-based materials are more likely to induce curvature in the system, just as phosphatidyl ethanolamines do in phospholipid bilayers.[42] Of course, this effect will be expected to become more pronounced in hydrated systems.

The xylose material, **5d**, unlike the other materials is not mesomorphic. This is probably due to the fact that the sugar unit has one less hydroxyl group in comparison to the galactose, glucose, and mannose systems. The extent of the intermolecular hydrogen bonding is thus less, and therefore, the interactions holding together any potential mesophase structure, i.e., at the interfaces between the layers in the lamellar phase or at the center of the column in a columnar phase, will be much reduced.

## 5. Conclusion

In conclusion, we have shown that a number of novel sugar-based azo-compounds exhibit mesomorphic behavior, and that a subtle change in stereochemistry, from equatorial- to axial-located hydroxyl groups, can tilt the balance from a lamellar phase to a columnar phase. This result may have implications for the way in which biomembranes are constructed.

**Acknowledgment.** We thank M.-N. Bouchu and J. A. Haley for technical assistance, the Centre National de la Recherche Scientique, the French Minister of Foreign Office, and the Ramsay Memorial Fund for financial support.

**Supporting Information Available:** Synthetic methods for the preparation of materials and experimental procedures for the evaluation of physical properties (PDF). This material is available free of charge via the Internet at http://pubs.acs.org.

JA037347X

(42) Andersson, A.-S.; Rilfors, L.; Bergqvist, M.; Persson, S.; Lindblom, G. *Biochemistry* **1996**, *35*, 11119−11130.